Angiogenic Deficiency and Adipose Tissue Dysfunction Are Associated with Macrophage Malfunction in SIRT1$^{-/-}$ Mice

Fen Xu, David Burk, Zhanguo Gao, Jun Yin, Xia Zhang, Jianping Weng, and Jianping Ye

Department of Endocrinology (F.X., J.W.), The Third Affiliated Hospital of Sun Yat-Sen University, Guangzhou 510630, China; Pennington Biomedical Research Center (D.B., Z.G., J.Yi., J.Ye), Louisiana State University System, Baton Rouge, Louisiana 70808; Department of Endocrinology and Metabolism (J.Yi.), Shanghai Jiao Tong University Affiliated Sixth People's Hospital, Shanghai 200233, China; and Department of Cell Biology and Molecular Genetics (X.Z.), University of Maryland, College Park, Maryland 20742

The histone deacetylase sirtuin 1 (SIRT1) inhibits adipocyte differentiation and suppresses inflammation by targeting the transcription factors peroxisome proliferator-activated receptor γ and nuclear factor κB. Although this suggests that adiposity and inflammation should be enhanced when SIRT1 activity is inactivated in the body, this hypothesis has not been tested in *SIRT1* null (*SIRT1*$^{-/-}$) mice. In this study, we addressed this issue by investigating the adipose tissue in *SIRT1*$^{-/-}$ mice. Compared with their wild-type littermates, SIRT1 null mice exhibited a significant reduction in body weight. In adipose tissue, the average size of adipocytes was smaller, the content of extracellular matrix was lower, adiponectin and leptin were expressed at 60% of normal level, and adipocyte differentiation was reduced. All of these changes were observed with a 50% reduction in capillary density that was determined using a three-dimensional imaging technique. Except for vascular endothelial growth factor, the expression of several angiogenic factors (*Pdgf*, *Hgf*, endothelin, apelin, and *Tgf-β*) was reduced by about 50%. Macrophage infiltration and inflammatory cytokine expression were 70% less in the adipose tissue of null mice and macrophage differentiation was significantly inhibited in *SIRT1*$^{-/-}$ mouse embryonic fibroblasts *in vitro*. In wild-type mice, macrophage deletion led to a reduction in vascular density. These data suggest that *SIRT1* controls adipose tissue function through regulation of angiogenesis, whose deficiency is associated with macrophage malfunction in *SIRT1*$^{-/-}$ mice. The study supports the concept that inflammation regulates angiogenesis in the adipose tissue. **(*Endocrinology* 153: 1706–1716, 2012)**

Mammalian sirtuin 1 (SIRT1) is a nicotinamide adenine dinucleotide^{+}-dependent class III histone deacetylase and is expressed in all cell types. SIRT1 plays an important role in the control of energy homeostasis in mammalians (1, 2), although its potential antiaging activity remains controversial. SIRT1 promotes energy expenditure and protects insulin sensitivity in diet-induced obese mice (3–5). In hepatocytes, SIRT1 reduces the risk of hepatic steatosis in transgenic mice (6, 7). Recent studies suggest that SIRT1 regulates angiogenesis and vascular function *in vivo* (8–11). SIRT1 is highly expressed in vascular cells and is required for endothelial cell proliferation (8), and its inactivation leads to inhibition of blood vessel development and vascular remodeling (8). Another study suggests that SIRT1 may inhibit angiogenesis by suppressing hypoxia inducible factor 1 alpha activity (11). Because angiogenesis is required for adipose tissue growth as well as for maintenance of adipose tissue function (12, 13), it

ISSN Print 0013-7227 ISSN Online 1945-7170
Printed in U.S.A.
Copyright © 2012 by The Endocrine Society
doi: 10.1210/en.2011-1667 Received August 23, 2011. Accepted January 4, 2012.
First Published Online February 7, 2012

Abbreviations: C/EBP, CCAAT/enhancer binding protein; 3D, three dimensional; FBS, fetal bovine serum; H&E, hematoxylin and eosin; KO, knockout; M1, M1-polarized macrophage; M2, M2-polarized macrophage; MEF, mouse embryonic fibroblast; NF-κB, nuclear factor κB; NMR, nuclear magnetic resonance; PDGF, platelet-derived growth factor; PPARγ, peroxisome proliferator-activated receptor γ; *Pref-1*, preadipocyte factor 1; SIRT1, sirtuin 1; VEGF, vascular endothelial growth factor; WAT, white adipose tissue; WT, wild type.

Downloaded from https://academic.oup.com/endo/article/153/4/1706/2423847 by guest on 23 April 2024

is not clear whether SIRT1 regulates adipose tissue function through angiogenesis.

SIRT1 was reported to inhibit ligand-dependent peroxisome proliferator-activated receptor γ (PPARγ) function in adipocytes (14). The study demonstrated that PPARγ activity was elevated in adipocytes in the absence of SIRT1. Although *SIRT1* null mice were reported in 2003 with small body size (15), the adipose tissues were not investigated in the mice. We expect that adipose tissue growth should be enhanced in *SIRT1*-deficient mice. In this study, we investigated the adipose tissue growth and function in *SIRT1* knockout (KO) (*SIRT1*$^{-/-}$) mice. This study represents our effort to elucidate the relationship between angiogenesis and adipose tissue function. We proposed that chronic adipose inflammation is a result of an obesity-induced hypoxic response, and inflammation is required for amplification of the hypoxia signal in the stimulation of angiogenesis (16, 17). In adipose tissue, angiogenesis controls adipocyte activities through vascular remodeling and maintenance of blood supply during adipose tissue expansion (18–21). Insufficient angiogenesis may lead to chronic inflammation through the hypoxia response in obesity (16, 17). Angiogenesis is regulated by proinflammatory cytokines and adipokines (leptin and adiponectin) (22, 23). Adipose macrophages stimulate angiogenesis through production of cytokines (23). In addition, the macrophages also act to remove dead adipocytes (24). However, the angiogenic activity of macrophages remains to be tested in multiple model systems. In this study, we examined the angiogenic function of macrophages in the adipose tissue of *SIRT1* null mice.

We analyzed the white adipose tissue (WAT) of *SIRT1*$^{-/-}$ mice and observed a significant reduction in adipocyte function. The adipocyte dysfunction is associated with angiogenic deficiency and macrophage malfunction in the tissue. The study suggests that SIRT1 may regulate adipose tissue function through macrophages, which controls angiogenesis through proinflammatory cytokines.

Materials and Methods

Animals

C57BL/6J breeders (4 wk in age) were obtained from The Jackson Laboratory (Bar Harbor, ME). *SIRT1*$^{+/-}$ mice on the 129/J background were a gift of Frederick W. Alt at the Howard Hughes Medical Institute, Children's Hospital, Center for Blood Research, and Department of Genetics (Harvard University Medical School, Boston, MA) (25). *SIRT1*$^{+/-}$ mice were backcrossed with C57BL/6 mice for nine generations to gain the C57BL/6 gene background. The heterozygous C57BL/6 breeders were used to produce *SIRT1*$^{-/-}$ mice. Wild-type (WT) littermates were used as the control. Breeders were housed in plastic boxes with corn-cob bedding in the animal facility at the Pennington Biomedical Research Center. Animal rooms were maintained at 22–24 C with a 12-h light, 12-h dark cycle. All procedures were performed in accordance with National Institutes of Health guidelines for the care and use of animals and approved by the Institute Animal Care and Use Committee at the Pennington Biomedical Research Center.

Nuclear magnetic resonance (NMR)

Body composition was measured using quantitative NMR as previously described (26). Briefly, conscious unrestrained mice were placed in small tubes and then inserted into a Brucker model mq10 NMR analyzer one at a time (Brucker, Milton, Ontario, Canada). The fat and lean mass were recorded within 1 min.

DNA preparation and genotyping PCR

DNA was prepared from tail samples using the proteinase K protocol. The genotyping PCR was conducted in all of the founders and their offspring. The genotyping PCR was performed using primers below, which were ordered from Sigma (St. Louis, MO):

SIRT1SKO-F, 5′-CTTGCACTTCAAGGGACCAA;
SIRT1SKO-R1, 5′-GTATACCCACCACATCTGAG;
SIRT1SKO-R2, 5′-CTACCACTCCTGGCTACCAA.

The reaction mixture contained: 200 ng of DNA, 0.5 μl of thermol buffer, 50 mM deoxynucleotide triphosphate, forward primers, reverse primers, and 2.5 U of TaqMan enzyme. PCR products were resolved in 1.2% agarose gel, and the DNA band was detected with a Bio-Rad (Hercules, CA) UV detector.

Mouse embryonic fibroblasts (MEF) and adipogenesis

MEF were prepared from 13-d embryos of the SIRT1$^{-/-}$ or WT mice as reported elsewhere (27). Embryos were minced and digested with trypsin after removal of the limbs, internal organs, and brain. After digestion at 37 C for 10 min, the cell suspension was collected and washed with DMEM supplemented with 10% newborn calf serum. The cells were plated in 100-mm cell culture plate in the serum-containing medium, and the medium was changed 24 h later. After one passage, the cells were collected as MEF. The SIRT1$^{-/-}$ MEF and WT MEF were confirmed by genotyping, then 5×10^4 cells/well were plated in six-well plates for an adipogenesis assay. The cells were maintained in 10% fetal bovine serum (FBS) containing 1 μM 3-isobutyl-1-methylxanthine, 10 μM dexamethasone, 10 μg/ml of insulin, and 1 μm of troglitazone for 4–6 d (media were changed every 2 d). The cells were then treated with medium supplemented with 10% FBS and 10 μg/ml insulin for 2 d to obtain mature adipocytes.

Vascular imaging

Adipose tissue staining was performed as described elsewhere (28). Mice were killed and then decapitated to remove blood. The tip portion of epididymal fat was collected under sterile condition and minced into small pieces (2–3 mm) using scissors. The fat tissue pieces were washed with 1× PBS once and then incubated in PBS containing both Griffonia simplicifolia IB4 isolectin Alexa Fluor 488 (40 μg/ml in PBS) to stain endothelial cells and BODIPY 558/568 (5 μM in PBS) for lipid staining overnight. The samples were washed three times in PBS (5–10 min per time) and fixed with 4% (wt/vol) formaldehyde for 24 h for long-term storage. Samples were kept in 1× PBS during the imaging process.

Downloaded from https://academic.oup.com/endo/article/153/4/1706/2423847 by guest on 23 April 2024

Confocal microscopy and image analysis

Vascular images were collected using a Zeiss (Jena, Germany) 510 META confocal with appropriate excitation lasers and band pass filters and equipped with a ×20 Plan-Apochromat objective (NA, 0.8). Image stacks were collected with a frame average of two and a step size of 0.76 μm. At least five randomly selected data stacks were collected for each sample. Generation of three-dimensional (3D) images was accomplished using Imaris (Bitplane, South Windsor, CT) version 6.2. Isosurface renderings of capillaries in each data stack were made using Imaris software and vessel volume determined with Imaris MeasurementPro. The total vessel volume in each sample was divided by the total tissue volume for the vascular density in each sample.

Macrophage differentiation and analysis

MEF were plated in a six-well plate at a density of 5×10^4 cells/well. The cells were differentiated into macrophages in a medium maintaining 10% FBS, 1 μM 3-isobutyl-1-methylxanthine, 10 μM dexamethasone, 10 μg/ml of insulin, and 1 μm of troglitazone for 4–6 d with a medium change every 2 d. The cells were then cultured in a medium containing 10% FBS and 10 μg/ml of insulin for 2 d. The differentiated cells were stained with florescent antibodies to macrophage marker proteins F4/80 (phycoerythrin) and CD11b (fluorescein isothiocyanate), and then analyzed using a flow cytometer.

Deletion of macrophages in adipose tissue

Macrophages were deleted in the adipose tissue by a single injection of clodronate liposome. Clodronate liposome was prepared and administration at 150 mg/kg ip as described elsewhere (29). The macrophage deletion was confirmed in adipose tissue at d 4 after injection via measurement of F4/80 mRNA expression levels.

Quantitative real-time PCR

Epididymal fat pad (for epididymal WAT) and brown adipose tissue were collected after a 6-h fast in mice and kept in liquid nitrogen. Total RNA was extracted from frozen tissues (kept at −80 C) using TRI Reagent (T9424; Sigma). TaqMan RT-PCR primer and probe were used to determine mRNA for adiponectin (Mm00456425_m1), leptin (Mm00434759_m1), preadipocyte factor 1 (*Pref-1*) (Mm00494477_m1), *ap2* (Mm00445880_m1), *Pparγ* (Mm00440945_m1), *Srebp-1* (Mm00550338_m1), *Cd31* (Mm00476702_m1), *Vegf-R2* (Mm00440099_m1), *Vegf* (Mm00437304_m1), *Pdgf* (Mm00440678_m1), apelin (Mn00443562-ml), endothelin (Mm00438656 -ml), *Hgf* (Mm01135177 _ml), *Tgf-β* (Mm00441724_m1), F4/80 (Mm00802530_m1), *Cd11b* (Mm00434455_m1), *Tnf-α* (Mm00443258_m1), *Il-1b* (Mm00434228_m1), *Il6* (Mm00446190_m1), *Mcp-1* (Mm00441242_m1), *iNos* (Mm00440485_m1), and arginase 1 (Mm00475988_ml). The reagents were purchased from Applied Biosystems (Foster City, CA). Mouse ribosome 18S rRNA_s1 (without intron-exon junction) was used as an internal control. Reactions were conducted using a 7900 HT Fast Real-Time PCR System (Applied Biosystems).

Western blotting

Whole-cell lysate was extracted from adipose tissue with sonication in lysis buffer and used in Western blotting as described elsewhere (30). Antibodies and their sources are as following: β-actin (ab6276; Abcam, Cambridge, MA), SIRT1 (DAM1514081; Millipore, Bedford, MA), sterol regulatory element binding protein 1 (F0906; Santa Cruz Biotechnology, Inc., Santa Cruz, CA), PPARγ (sc-7273; Santa Cruz Biotechnology, Inc.), and CCAAT/enhancer binding protein (C/EBP)α (sc-61X; Santa Cruz Biotechnology, Inc.). To detect multiple signals from one membrane, the membrane was stripped with a stripping buffer.

Immunohistochemistry

Fresh epididymal fat pads were isolated, fixed in neutral buffered formalin, dehydrated, and embedded in paraffin. Thin tissue slides (5 μm) were deparaffinized, blocked, and incubated overnight at 4 C with mouse antimouse CD31 antibody (ab24590; Abcam) and mouse antirat F4/80 (sc-71087; Santa Cruz Biotechnology, Inc.), which was followed by signal amplification using a VECTASTAIN Elite ABC kit (PK-6102; Vector Laboratories, Burlingame, CA). The reaction was developed by addition of AEC chromogen substrate (AEC Staining kit; Sigma-Aldrich, St. Louis, MO). Microphotographs were taken under a microscope (×20).

Hematoxylin and eosin (H&E) staining

Fresh fat tissues were collected at 28 wk of age and fixed in 10% neutral buffered formalin solution (HT50-1-2; Sigma). The tissue slides were obtained through serial cross-section cutting at 8-μm thickness and processed with a standard procedure.

Oil red-O staining

Accumulation of triglyceride content in differentiated MEF cells was visualized by staining with Oil red-O (Sigma-Aldrich). Briefly, a stock solution of 0.5% (wt/vol) Oil red-O was prepared in isopropanol. To achieve a working concentration (60%), 12 ml of stock solution were mixed with 8 ml of water and filtered with 0.2-μm filter. The cells were first fixed using 10% neutral buffered formalin for 1 h, washed with 60% isopropanol, air dried, stained with Oil red-O working solution for 10 min, and then washed with dH_2O four times or under running tap water. The triglyceride accumulation was photographed with a Nikon microscope (Eclipse TS100; Nikon, Tokyo, Japan). The stain was eluted by incubation with 750 μl (depending on well size) of isopropanol, and its intensity was determined by light absorption at 500 nm with a microplate reader.

Statistical analysis

In this study, the data were presented as mean ± SEM from multiple samples; n = 3–7 for each group in animal study. All of the *in vitro* experiments were conducted at least three times. Two-tailed, unpaired Student's *t* test was used in the statistical analysis with significance $P \leqslant 0.05$.

Results

Adipose tissue of *SIRT1*$^{-/-}$ mice

In this study, *SIRT1* null (*SIRT1*$^{-/-}$) mice were produced from the heterozygous (*SIRT1*$^{+/-}$) breeder in C57BL/6 gene background and maintained on the regular chow diet. The null mice died frequently in the postnatal period from starvation likely due to their inability to compete with their WT littermates of normal size for milk. We

Downloaded from https://academic.oup.com/endo/article/153/4/1706/2423847 by guest on 23 April 2024

reduced the competition by removing some of the normal littermates to keep four pups in total per litter. In the phenotype study, *SIRT1* null mice were compared with the WT littermates at 28 wk in age. The null mice had a 50% reduction in body weight and fat mass when compared with their WT littermates (Fig. 1A). The difference in body size was not apparent at birth but developed after birth and remained throughout adulthood. The epididymal fat (white fat) and brown fat were isolated and appeared to be much smaller in KO mice (Fig. 1, B and C). Although *SIRT1*$^{-/-}$ mice exhibited a 50% reduction in body weight and fat content when compared with WT animals (Fig. 1D), their ratio of fat mass to body weight was comparable with that of WT mice (~22%), suggesting that the fat content is normal in the null mice.

Decrease in adipocytes size, extracellular matrix, and adipokine expression in *SIRT1*$^{-/-}$ mice

The WAT was further investigated using the epididymal fat tissue in this study. Histological analysis was conducted after H&E staining of the fat tissue. *SIRT1*$^{-/-}$ mice exhibited a significant reduction in adipocytes size and extracellular matrix (Fig. 2A). The tissue appeared to exhibit a decrease in the heterogeneity of cell size (Fig. 2A). Adipocytes appeared to be smaller with a decrease in the variability of cell diameters typically observed in WT adipose tissue. There was also a decrease in the amount of extracellular matrix around the adipocytes of KO animals as evidenced by the reduction in eosin positive staining between individual cells, suggesting a higher cellular density in the adipose tissue. Expression of adipokines and adipocyte-enriched transcription factors were examined to characterize the change in adipose tissue in SIRT$^{-/-}$ animals. Expression of adiponectin (*Acdc*) and leptin mRNA was much lower in the null mice (Fig. 2B), whereas *Pref-1* expression was higher (Fig. 2B). This gene expression profile suggests a decrease in adipocyte differentiation and an increase in preadipocytes density in the adipose tissue. Expression of *ap2*, *Pparγ*, and *Srebp* was not changed in the null mice (Fig. 2B), suggesting that the adipogenic transcriptional program is not deficient in the

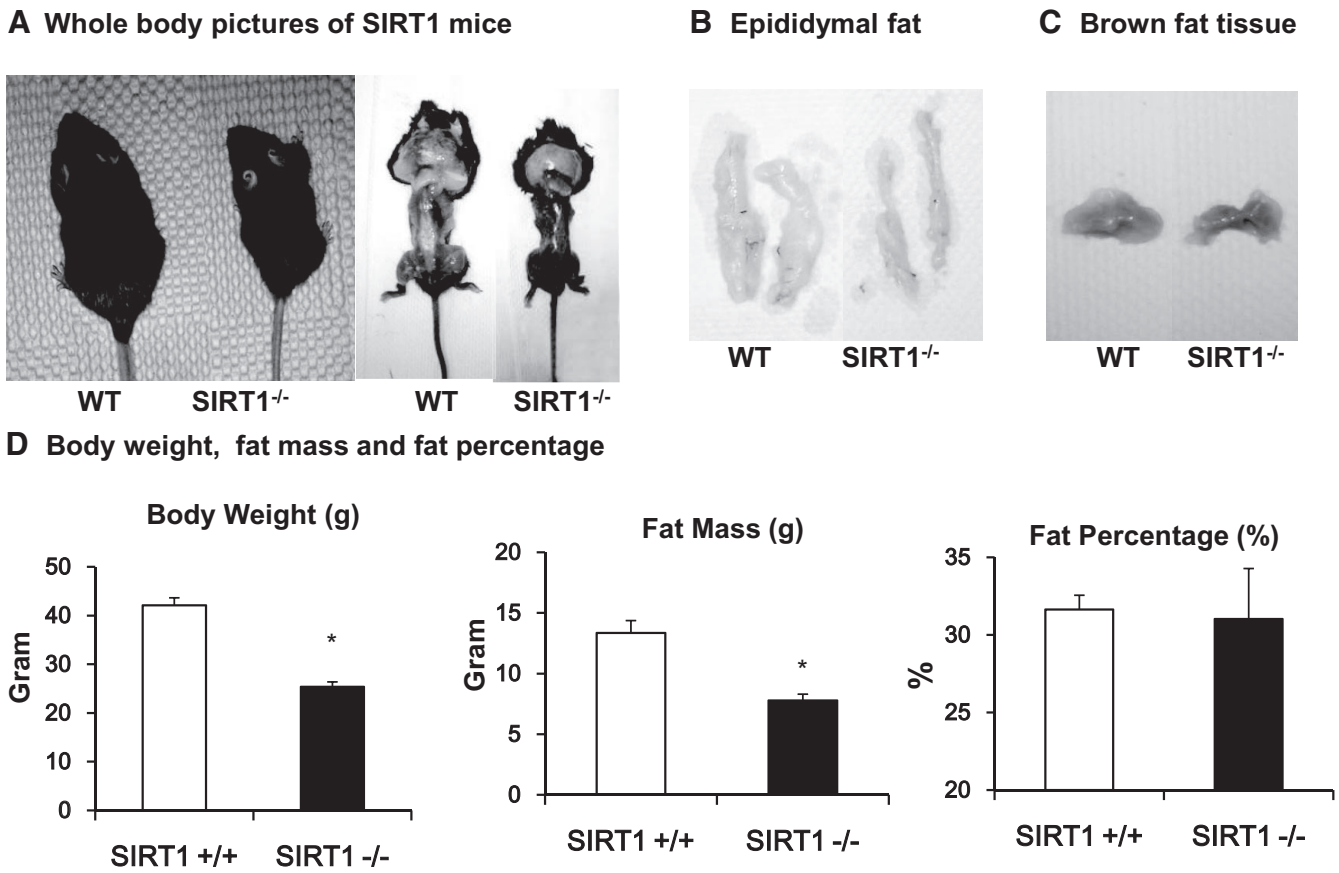

FIG. 1. Adipose tissue in *SIRT1*$^{-/-}$ mice. Mice were fed chow diet for 28 wk and then used in tissue collection. A, Comparison of WT and SIRT1$^{-/-}$ before and after killing. B, WAT of epididymal fat pad. C, Brown adipose tissue. D, Body weight, fat mass, and body composition. Data are from animals fed chow diet for 22 wk. Measurements were conducted after an overnight fast. The fat mass was determined using whole-body NMR. The fat percentage in the body composition was determined by the ratio of fat mass to body weight. In this figure, each value represents the means ± SE (n = 7). *, $P \leq 0.05$.

Downloaded from https://academic.oup.com/endo/article/153/4/1706/2423847 by guest on 23 April 2024

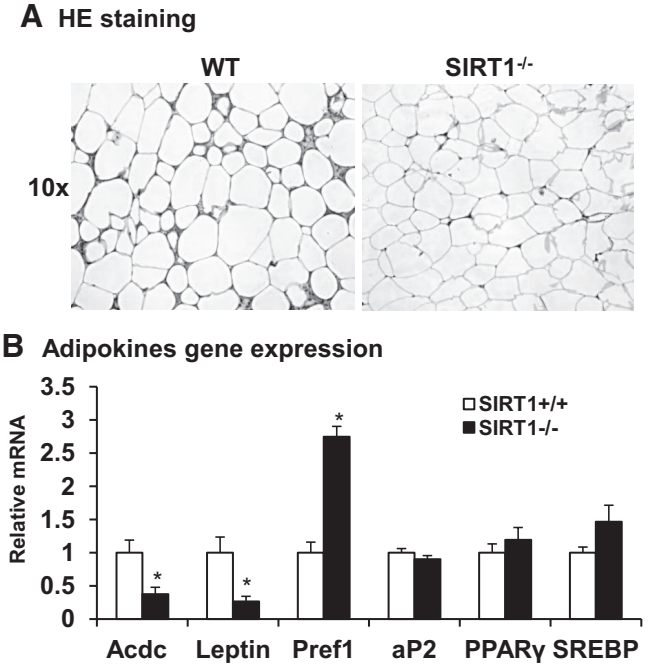

FIG. 2. Structural and functional analysis of adipose tissue. A, Microscopic view of adipose tissue. Epididymal adipose tissue was collected at 28 wk of age and subjected to H&E staining. The pictures represent the histology of adipose tissue in the *SIRT1* null and WT mice. B, Adipokine gene expression. Gene expression was determined in mRNA for the key genes in adipocytes by quantitative RT-PCR. Values are the means ± SE (n = 6). *, $P \leq 0.05$.

tissue. However, adipocytes are impaired in adipogenesis, lipid storage, and endocrine functions in the adipose tissue of null mice. The reduction in extracellular matrix suggests that the adipocyte dysfunction is likely a result of a micro environment abnormality in the adipose tissue.

Adipogenesis *in vitro*

SIRT1 was reported to inhibit PPARγ function promoting lipid mobilization in adipocytes (14). With this in mind, PPARγ function should be enhanced and adipogenesis should be promoted in *SIRT1* null mice. This rationale is challenged by the data that adipogenesis is actually reduced in the null mice. To understand the difference, we reviewed literature about regulation of adipogenesis in adipose tissue. Adipogenesis is determined by preadipocyte quality and the differentiation environment. To determine which factor plays a role in the altered adipogenesis in *SIRT1* null mice, we examined adipocyte differentiation potential *in vitro*. MEF cells were prepared from a 13-d embryo and induced for adipogenesis in the culture medium as described in *Materials and Methods*. The differentiation was determined by quantification of lipid accumulation and gene expression. Compared with WT cells, lipid accumulation in differentiated cells from *SIRT1*$^{-/-}$ MEF was enhanced as observed by the red color from the Oil red-O staining (Fig. 3A). An increase was also

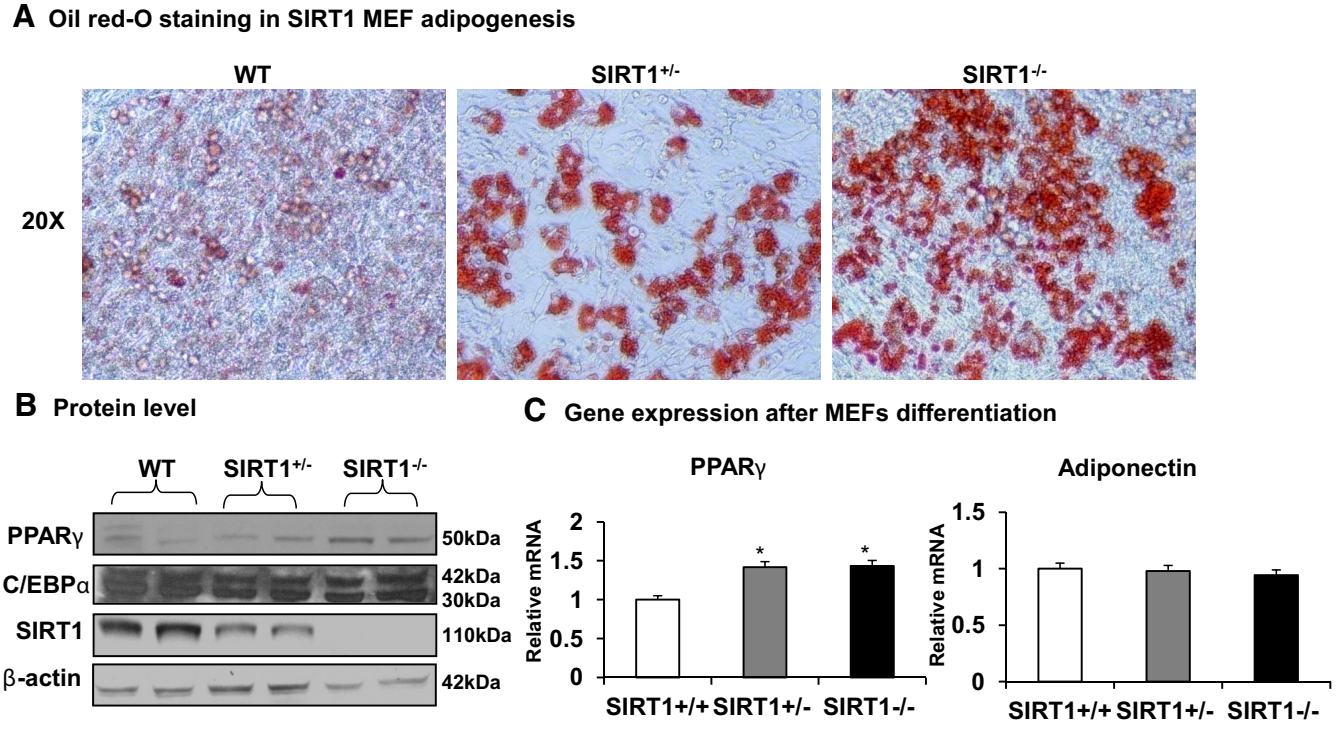

FIG. 3. Adipogenesis *in vitro*. MEF were generated and differentiated into adipocytes *in vitro*. Differentiation was determined with Oil red-O staining and gene expression. A, Oil red-O staining of lipid in differentiated cells. Lipid is indicated by the *red color* in the cytoplasm. Heterozygous KO MEF (*SIRT1*$^{+/-}$) were used in the control together with WT MEF. B, PPARγ and C/EBPα protein in differentiated cells. The proteins were determined in Western blotting. C, mRNA of PPARγ and adiponectin in differentiated cells. Values are the means ± SE (n = 6). *, $P \leq 0.05$.

Downloaded from https://academic.oup.com/endo/article/153/4/1706/2423847 by guest on 23 April 2024

observed in the heterozygous ($SIRT1^{+/-}$) MEF (Fig. 3A) and suggests an increased adipogenic potential in *SIRT1*-deficient cells. To understand the molecular basis of adipogenesis, we examined two transcription factors (PPARγ and C/EBPα) that are required for adipocyte differentiation. After differentiation, $SIRT1^{-/-}$ cells exhibited a modest elevation in mRNA and protein for *PPARγ* but not for *C/EBPα* (Fig. 3, B and C). There was no significant change in adiponectin expression in $SIRT1^{-/-}$ adipocytes (Fig. 3C). The results suggest that $SIRT1^{-/-}$ preadipocytes are not deficient, because they differentiated very well *in vitro*. The result suggests a defect in the microenvironment in the adipose tissue of $SIRT1^{-/-}$ mice. Additionally, the lipid accumulation and gene expression suggest that PPARγ function is enhanced in $SIRT1^{-/-}$ adipocytes.

Reduced capillary density and impaired angiogenesis in epididymal fat of $SIRT1^{-/-}$ mice

The extracellular matrix provides the microenvironment to adipocytes in adipose tissue. In the extracellular matrix, the vascular system determines blood supply, and the collagen network controls the space for adipocyte size expansion (31). Angiogenesis is a process of new capillary formation that extends the existing vascular system in growing tissues. In the body, an increase in angiogenesis accompanies adipose tissue growth (18–21). Angiogenesis was examined in the adipose tissue of SIRT1 null mice to understand the cause of adipogenic deficiency. Capillaries were stained in fresh adipose tissue with isolectin that binds to endothelial cells in the capillary. To quantify the capillary density, the fluorescent signal was collected using a confocal microscope at multiple z-planes in the tissue and used to generate 3D reconstructions of the labeled cell types as described in *Materials and Methods* (Fig. 4A). In the 3D image, adipocytes are in red color and capillaries are green. The images show that the adipose tissue has a rich capillary network, and each adipocyte has more than one capillary on average. After exclusion of adipocytes, a clean capillary network was generated, and this was used to calculate vascular volume (Fig. 4B). Vascular volume was then divided by the total tissue volume for normalization. Our measurements show that the cap-

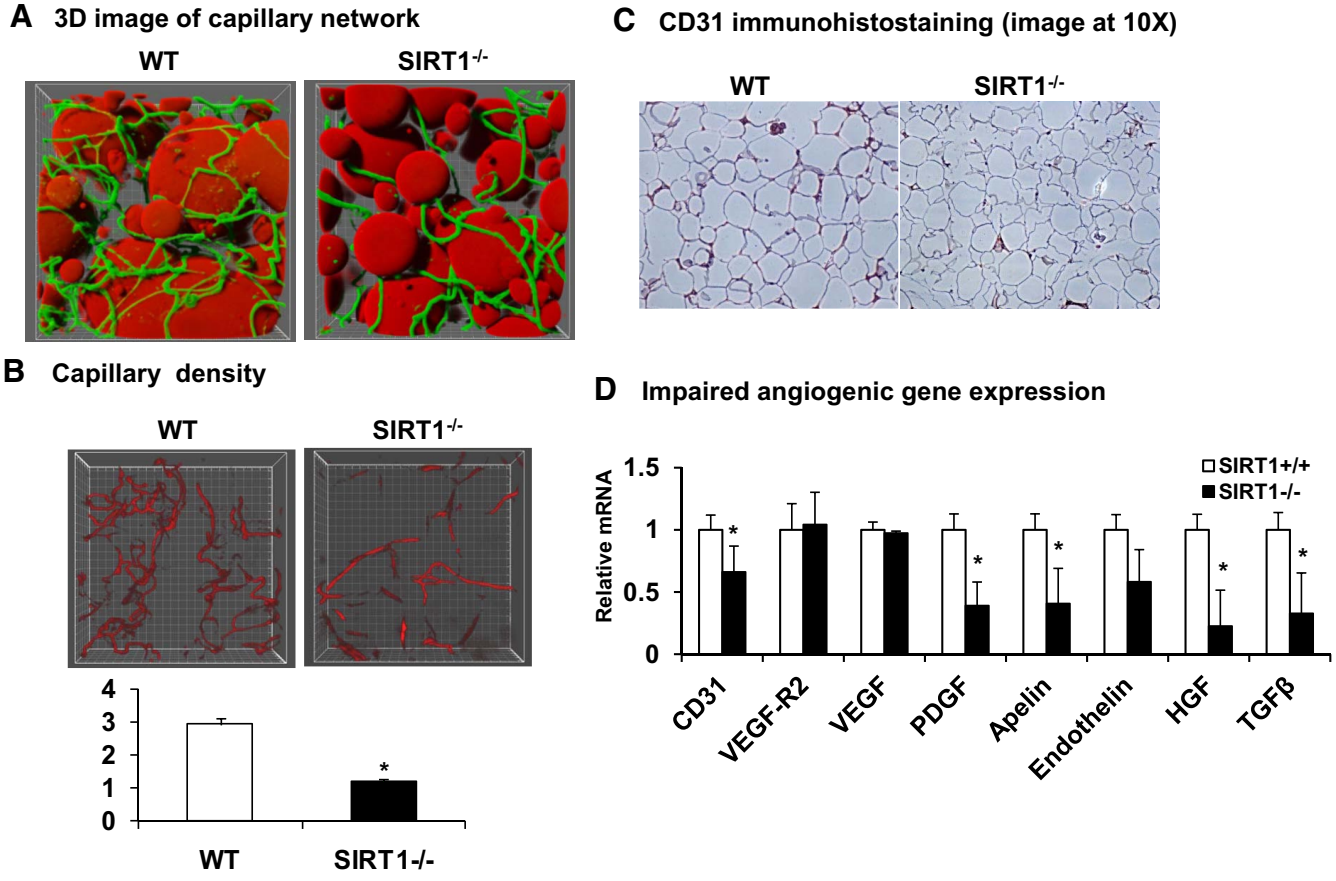

FIG. 4. Capillary density in adipose tissue of $SIRT1^{-/-}$ mice. A, 3D image of adipose tissue capillaries. The images were generated as described in *Materials and Methods*. The *round objects in red color* represent adipocytes. The *green lines* are capillaries. B, Capillary density. The total vessel volume is divided by the total stack volume to obtain capillary density. C, CD31 immunohistostaining in fat tissue. D, Angiogenic gene expression in epididymal fat tissue. Relative mRNA expression of key angiogenic genes was determined. Values are the means ± SE (n = 6). *, $P \leq 0.05$.

Downloaded from https://academic.oup.com/endo/article/153/4/1706/2423847 by guest on 23 April 2024

illary density was reduced by 50% in the adipose tissue of *SIRT1*$^{-/-}$ mice (Fig. 4B). When the capillary density was determined by the endothelial cell marker CD31 in immunohistostaining, a 40% reduction was observed in *SIRT1*$^{-/-}$ mice (Fig. 4C). These data consistently suggest that the capillary density is reduced in the adipose tissue of *SIRT1* null mice.

Angiogenesis is regulated by a balance between the proangiogenic and antiangiogenic factors. Expression of angiogenic factors and their receptors were examined in the fat tissue to understand the molecular basis of the capillary reduction (Fig. 4D). Expression of angiogenic factors, including *Pdgf*, apelin, endothelin, *Hgf*, and *Tgf-β*, were reduced in *SIRT1* null mice as well as mRNA expression of the endothelial marker, CD31. *Vegf* and *Vegf-r* were not reduced in the tissue (Fig. 4D). These data suggest that *SIRT1* null mice suffer angiogenic deficiency from lack of angiogenic factors.

Decreased macrophage activity in fat tissue of *SIRT1*$^{-/-}$ mice

Macrophages are a major source of both angiogenic factors and proinflammatory cytokines in adipose tissue (22, 23). Stimulation of angiogenesis is one of the macrophage functions in response to hypoxia (23). We were not sure whether the angiogenic deficiency observed in this study is related to a change in the macrophage activities in the adipose tissue of *SIRT1* null mice. To address this question, we examined macrophage infiltration and expression of inflammatory genes in adipose tissue. Relative macrophage abundance was determined by the mRNA expression level of macrophage markers, *F4/80* and *CD11*. Levels of both gene transcripts were reduced by 70–80% in the tissue of *SIRT1* null mice (Fig. 5, A and B), and expression of *Tnf-α*, *Mcp-1*, and *Il-1β* that are mainly secreted by macrophages was also reduced in the tissue (Fig. 5, C–E). *iNos* is primarily expressed in M1-polarized macrophage (M1) and arginase 1 is highly expressed in M2-polarized macrophage (M2) (32, 33). mRNA levels of both genes were decreased by more than 60% in *SIRT1*$^{-/-}$ mice (Fig. 5, F and G), suggesting that the numbers of both M1 and M2 macrophages were decreased in the adipose tissue of *SIRT1* null mice. Expression of *Il-6* was not significantly altered by SIRT1 inactivation (Fig. 5H). Macrophage infiltration was also determined using F4/80 pro-

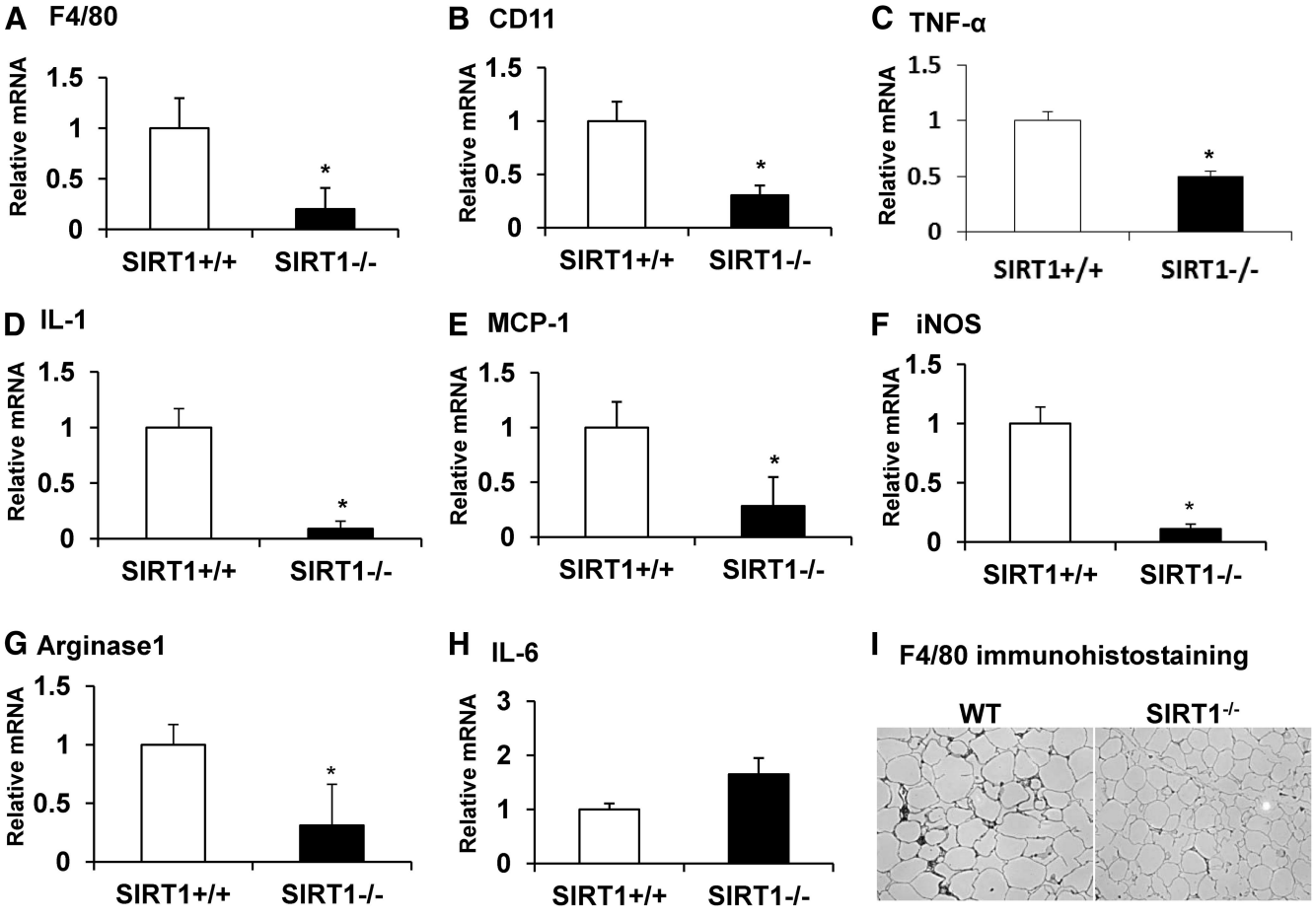

FIG. 5. Decreased macrophage activity in fat tissue of *SIRT1*$^{-/-}$ mice. Gene expression was determined using quantitative RT-PCR. A–H, Relative levels of mRNA in adipose tissue. I, Immunostaining of macrophage marker F4/80 in adipose tissue. Values are the means ± SE (n = 6). *, $P \leq 0.05$.

Downloaded from https://academic.oup.com/endo/article/153/4/1706/2423847 by guest on 23 April 2024

tein in the tissue. The immunohistological staining suggests that F4/80 protein was reduced in the fat tissue of *SIRT1*$^{-/-}$ mice (Fig. 5I). This group of data suggests that macrophage activities are decreased in the adipose tissue of *SIRT1*$^{-/-}$ mice and may contribute to the decreased angiogenic activity in *SIRT1*$^{-/-}$ mice.

Macrophage differentiation and deletion in adipose tissue

A reduction in macrophage differentiation may occur in *SIRT1*$^{-/-}$ mice because M2 macrophages were reduced in the adipose tissue. The M2 reduction explains the M1 reduction because M2 is the precursor of M1. To test this possibility, we examined macrophage differentiation from *SIRT1*$^{-/-}$ MEF. The differentiation was induced *in vitro* and determined with protein expression of the macrophage marker genes, F4/80 and CD11b. The positive cells for the two markers were quantified using the flow cytometry. The result suggests that macrophage differentiation was reduced 50% in *SIRT1*$^{-/-}$ cells (Fig. 6A).

To prove the role of macrophages in the control of adipose tissue angiogenesis, we deleted macrophages in adipose tissue and then examined capillary density in WT mice using a single injection of clodronate liposome to deplete macrophages. Both capillary volume and capillary density were quantified using the 3D imaging technology. The macrophage deletion led to a decrease in both parameters in the fat tissue (Fig. 6, B and C). Expression of *F4/80* was reduced by 90% in adipose tissue, suggesting that macrophage deletion was achieved successfully (Fig. 6D). These data suggest that macrophage inhibition leads to angiogenic suppression in the adipose tissue.

Discussion

This study provides a novel mechanism, by which SIRT1 regulates adipocyte function. SIRT1 regulates fatty acid metabolism in adipocytes and hepatocytes, promotes lipid mobilization in adipocytes (14), stimulates fatty acid export in hepatocytes (6), and drives fatty acid oxidation in the mitochondria of hepatocytes (7). At the molecular level, SIRT1 regulates gene transcription by inhibiting PPARγ and activating peroxisome proliferator-activated receptor gamma coactivaor-1α. SIRT1 is a corepressor in the regulation of transcription factors such as PPARγ in adipocytes, and the PPARγ function should be enhanced after the corepressor inhibition by *SIRT1* KO in adipocytes. *SIRT1* null mice should exhibit an increased adiposity as a result of enhanced PPARγ function. However, this prediction is challenged by the phenotype of *SIRT1* null mice, which did not exhibit an increase in body fat. Their adipose tissue exhibited reduced levels of adipogenesis and adipokine (leptin and adiponectin) expression. Histological analysis suggests that they exhibited a lower number of small adipocytes (an indicator of adipogenesis and new adipocytes). There were more preadipocytes in their adipose tissue as indicated by the elevated *Pref-1* mRNA. Interestingly, the reduced differentiation was only observed *in vivo* but not *in vitro*. When adipocyte differentiation was tested in cell culture, no reduction was observed in *SIRT1* null MEF, suggesting that the adipogenic inhibition is derived from the microenvironment in their adipose tissue. Our data suggest that SIRT1 regulates adipocyte activity through modification of the extracellular environment.

Macrophage activities are decreased in the adipose tissue of *SIRT1* null mice. We examined the microenvironment by monitoring macrophage activities in the adipose tissue to understand the mechanism of adipogenic inhibition in

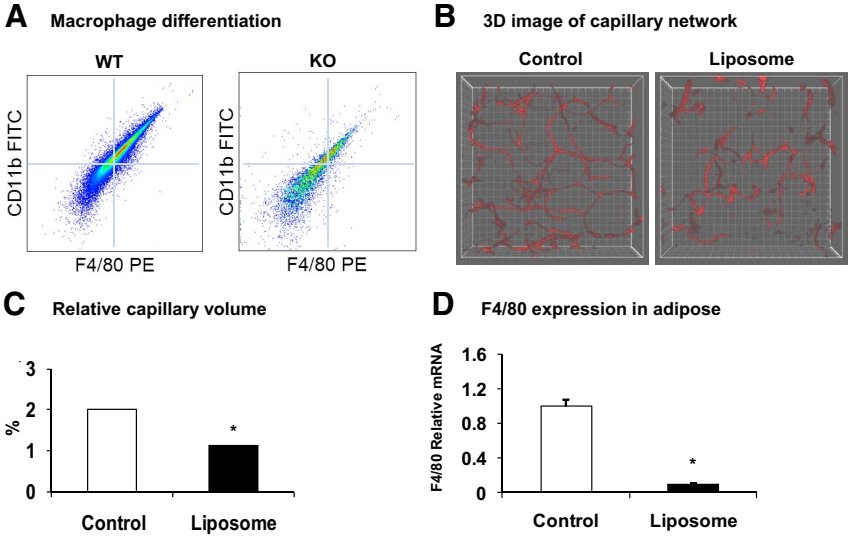

FIG. 6. Macrophage differentiation and macrophage deletion. A, Macrophage differentiation *in vitro*. Macrophages were differentiated from MEF *in vitro* and analyzed for expression of F4/80 and CD11b using flow cytometry. The figure presents the cell population (signal intensity) of double positive cells in WT and KO cells after differentiation. B, Capillary density after macrophages deletion. Macrophages were deleted in the adipose tissue of C57BL/6J mice on chow diet at 12 wk of age with one injection of clodronate liposomes (150 mg/kg). The control mice were injected with PBS. The fat tissue was collected and examined at d 4 after injection. A 3D image of the capillary network from the tip section of epididymal fat is shown. C, Quantification of relative capillary density. The relative capillary density was determined by ratio of capillary volume to fat mass volume. D, Macrophages in adipose tissue after deletion. F4/80 mRNA levels were determined to confirm macrophage deletion. In the *bar* figure, each data points represents mean ± SE (n = 3). *, $P \leq 0.05$. PE, Phycoerythrin.

Downloaded from https://academic.oup.com/endo/article/153/4/1706/2423847 by guest on 23 April 2024

SIRT1 null mice. SIRT1 was reported to inhibit inflammation by suppressing transcription factor nuclear factor κB (NF-κB) and activator protein 1 (27, 34, 35). In obese mice, SIRT1 inhibits inflammation through suppression of NF-κB in macrophages (5, 35). According to these reports, we expected that inflammation would be enhanced in the adipose tissue of *SIRT1* null mice but found the opposite in our current study. In adipose tissue, macrophage infiltration (*F4/80* and *CD11b positive cells*) was reduced, and this explains the decreased expression of proinflammatory genes (*Tnf-α*, *Il-1*, *Mcp-1*, and *iNos*). Both type 1 (M1, proinflammatory) and type 2 (M2, antiinflammatory) macrophages are decreased according to mRNA expression of *iNos* (M1 marker) and arginase 1 (M2 marker). These data suggest a deficiency in macrophage differentiation. To test this possibility, we examined macrophage differentiation *in vitro* using MEF cells. The differentiation was significantly inhibited in *SIRT1* null MEF according to the cell population analysis by flow cytometry. The data suggest that SIRT1 function is required for the differentiation process between the stem cells and macrophages. In a recent study, SIRT1 was inactivated in macrophages using lysozyme promoter-controlled Cre mice (36). In the conditional KO mice, macrophages exhibited an increase in inflammatory activities via an enhanced NF-κB activity. However, macrophage differentiation was not altered. The reason for this discrepancy between that and the current study is not clear. It is possible that the lysozyme Cre-mediated KO occurs at a later stage in the macrophage differentiation process, where SIRT1 activity is no longer required for macrophage differentiation.

The current study suggests that SIRT1 may regulate adipose angiogenesis through macrophages. SIRT1 was reported to influence angiogenesis by regulation of endothelial proliferation and endothelial cell differentiation in the process of vascular formation (8). It was not known whether SIRT1 acts in other cell types in addition to endothelial cells in the regulation of angiogenesis. This question is addressed in the current study. Capillary density was significantly reduced in the fat tissue of *SIRT1* null mice, and the reduction was associated with macrophage deficiency. To test the role of macrophages, we examined capillary density after macrophage deletion in mice. The relationship of macrophage deletion and capillary reduction supports our hypothesis that macrophage deficiency contributes to the angiogenic defect in the adipose tissue of *SIRT1* null mice. In addition to differentiation, cell apoptosis may be another factor contributing to the macrophage reduction in *SIRT1* null mice. SIRT1 inhibits cell apoptosis through suppression of transcription factor forkhead box O3 (37, 38) or p53 activity (39), which promotes cell apoptosis after activation. Dysregulation of these transcription factors may lead to elevation in macrophage apoptosis. The current study suggests that macrophages mediate SIRT1 activity in the regulation of angiogenesis. This conclusion is consistent with other reports demonstrating that macrophages are required for angiogenesis in adipose tissue (23, 28, 40). The study suggests a new mechanism by which SIRT1 regulates angiogenesis.

Vascular endothelial growth factor (VEGF) may not be involved in the angiogenic deficiency in *SIRT1*$^{-/-}$ mice. In the investigation of the molecular mechanisms of angiogenic deficiency, we examined mRNA expression of several angiogenic factors (41), such as *Vegf*, *Pdgf*, leptin (42, 43), adiponectin (44, 45), apelin, *Hgf*, and *Tgf-β*. In *SIRT1*$^{-/-}$ mice, most of those angiogenic factors except *Vegf* were reduced in the adipose tissue. Although VEGF is the most well-known angiogenic factor (31, 41), VEGF expression may not be critical in the angiogenic deficiency in *SIRT1*$^{-/-}$ mice. In addition to its expression, interaction with its receptor also plays a role in the control of VEGF activity. Platelet-derived growth factor (PDGF) is known to regulate VEGF activity at this level (46). PDGF regulates angiogenesis by recruiting and priming pericytes (47). In obese mice, a reduction in PDGF is associated with capillary reduction in adipose tissue (23). Adipokines also regulate capillary formation. For example, leptin stimulates endothelial cells to form capillaries in cell culture (42) and induces angiogenesis in a mouse corneal angiogenesis assay (43). Adiponectin stimulates angiogenesis, and this activity is related to cross talk between AMP-activated protein kinase and Akt signaling in endothelial cells (44). Apelin induces endothelial cell proliferation (48), and TGF-β stabilizes the new vessels (41). In *SIRT1* null mice, the reduction in all of these cytokines contributes to the angiogenic deficiency observed in adipose tissue. Adipose tissue contains adipocytes, macrophages, and endothelial cells, which secrete angiogenic factors. In *SIRT1* null mice, macrophage deficiency may account for a large part of the angiogenic factor reduction, but adipocytes and endothelial cells may contribute to the reduction as well.

We used 3D imaging techniques in the quantification of capillary density in fat tissue. In this method, capillary endothelial cells in fresh tissue are stained with a fluorescently conjugated isolectin, and the fluorescent signal is collected at multiple layers in the tissue using confocal microscopy. The reconstructed 3D image is generated using a computer program, and capillary volume is measured and normalized using the total tissue volume examined. We compared this technique with traditional immunohistostaining with CD31 antibody and obtained comparable results. The advantage of 3D imaging techniques is that it is more efficient and more accurate in the

Downloaded from https://academic.oup.com/endo/article/153/4/1706/2423847 by guest on 23 April 2024

quantification of capillary density and is much less labor intensive than other, more traditional, methods.

In this study, we analyzed adipose tissue in *SIRT1* null mice using histological techniques, measurements of gene expression, and measures of adipocyte differentiation. The results show that adipose tissues from null animals have small adipocytes and less extracellular matrix between adipocytes. The adipocytes exhibit a relatively homogeneous size distribution, and they express less adiponectin and leptin. Adipogenesis is reduced in the adipose tissue from lack of angiogenesis. Macrophage activities are reduced in the adipose tissue as indicated by the expression of macrophage marker genes, angiogenic factors, and inflammatory cytokines. The mechanism responsible for the down-regulation of macrophage activity remains to be elucidated, but cell apoptosis may play a role. Our data support that SIRT1 may control energy metabolism through the regulation of macrophage functions in adipose tissue.

Acknowledgments

Address all correspondence and requests for reprints to: Jianping Ye, 6400 Perkins Road, Baton Rouge, Louisiana 70808. E-mail: yej@pbrc.edu; or Jianping Weng, The Third Affiliated Hospital, Sun Yat-Sen University, Guangzhou 510630, China. E-mail: wjianp@mail.sysu.edu.cn.

This work was supported by National Institutes of Health (NIH) Grants DK068036 and DK085495 (to J.Ye) and by the Program for Changjiang Scholars and Innovative Research Team in the Sun Yat-Sen University (985 Project IRT0947) and National Natural Science Funds for Distinguished Young Scholar of China (Grant No. 81025005) (to J.W.). F.X. was supported by a scholarship from the China Scholarship Council (2007–2009). The quantitative RT-PCR and image data were obtained by using the Genetic Core and Bioimaging Core that are supported in part by Center of Biomedical Research Excellence (COBRE) (NIH 2P20RR021945) and Nutrition Obesity Research Center (NORC) (NIH 2P30DK072476) center grants from the NIH.

Disclosure Summary: The authors have nothing to disclose.

References

1. **Bordone L, Guarente L** 2005 Calorie restriction, SIRT1 and metabolism: understanding longevity. Nat Rev Mol Cell Biol 6:298–305
2. **Guarente L** 2006 Sirtuins as potential targets for metabolic syndrome. Nature 444:868–874
3. **Banks AS, Kon N, Knight C, Matsumoto M, Gutiérrez-Juárez R, Rossetti L, Gu W, Accili D** 2008 SirT1 gain of function increases energy efficiency and prevents diabetes in mice. Cell Metab 8:333–341
4. **Feige JN, Lagouge M, Canto C, Strehle A, Houten SM, Milne JC, Lambert PD, Mataki C, Elliott PJ, Auwerx J** 2008 Specific SIRT1 activation mimics low energy levels and protects against diet-induced metabolic disorders by enhancing fat oxidation. Cell Metab 8:347–358
5. **Pfluger PT, Herranz D, Velasco-Miguel S, Serrano M, Tschöp MH** 2008 Sirt1 protects against high-fat diet-induced metabolic damage. Proc Natl Acad Sci USA 105:9793–9798
6. **Xu F, Gao Z, Zhang J, Rivera CA, Yin J, Weng J, Ye J** 2010 Lack of SIRT1 (mammalian sirtuin 1) activity leads to liver steatosis in the SIRT1$^{+/-}$ mice: a role of lipid mobilization and inflammation. Endocrinology 151:2504–2514
7. **Purushotham A, Schug TT, Xu Q, Surapureddi S, Guo X, Li X** 2009 Hepatocyte-specific deletion of SIRT1 alters fatty acid metabolism and results in hepatic steatosis and inflammation. Cell Metab 9:327–338
8. **Potente M, Ghaeni L, Baldessari D, Mostoslavsky R, Rossig L, Dequiedt F, Haendeler J, Mione M, Dejana E, Alt FW, Zeiher AM, Dimmeler S** 2007 SIRT1 controls endothelial angiogenic functions during vascular growth. Genes Dev 21:2644–2658
9. **Potente M, Dimmeler S** 2008 Emerging roles of SIRT1 in vascular endothelial homeostasis. Cell Cycle 7:2117–2122
10. **Ota H, Eto M, Ogawa S, Iijima K, Akishita M, Ouchi Y** 2010 SIRT1/eNOS axis as a potential target against vascular senescence, dysfunction and atherosclerosis. J Atheroscler Thromb 17:431–435
11. **Lim JH, Lee YM, Chun YS, Chen J, Kim JE, Park JW** 2010 Sirtuin 1 modulates cellular responses to hypoxia by deacetylating hypoxia-inducible factor 1α. Mol Cell 38:864–878
12. **Cao Y** 2010 Adipose tissue angiogenesis as a therapeutic target for obesity and metabolic diseases. Nat Rev Drug Discov 9:107–115
13. **Cao Y** 2007 Angiogenesis modulates adipogenesis and obesity. J Clin Invest 117:2362–2368
14. **Picard F, Kurtev M, Chung N, Topark-Ngarm A, Senawong T, Machado De Oliveira R, Leid M, McBurney MW, Guarente L** 2004 Sirt1 promotes fat mobilization in white adipocytes by repressing PPAR-γ. Nature 429:771–776
15. **McBurney MW, Yang X, Jardine K, Hixon M, Boekelheide K, Webb JR, Lansdorp PM, Lemieux M** 2003 The mammalian SIR2α protein has a role in embryogenesis and gametogenesis. Mol Cell Biol 23:38–54
16. **Ye J** 2011 Adipose tissue vascularization: its role in chronic inflammation. Curr Diabetes Rep 11:203–210
17. **Ye J** 2009 Emerging role of adipose tissue hypoxia in obesity and insulin resistance. Int J Obes 33:54–66
18. **Rupnick MA, Panigrahy D, Zhang CY, Dallabrida SM, Lowell BB, Langer R, Folkman MJ** 2002 Adipose tissue mass can be regulated through the vasculature. Proc Natl Acad Sci USA 99:10730–10735
19. **Fukumura D, Ushiyama A, Duda DG, Xu L, Tam J, Krishna V, Chatterjee K, Garkavtsev I, Jain RK** 2003 Paracrine regulation of angiogenesis and adipocyte differentiation during in vivo adipogenesis. Circ Res 93:e88–97
20. **Neels JG, Thinnes T, Loskutoff DJ** 2004 Angiogenesis in an in vivo model of adipose tissue development. FASEB J 18:983–985
21. **Bråkenhielm E, Cao R, Gao B, Angelin B, Cannon B, Parini P, Cao Y** 2004 Angiogenesis inhibitor, TNP-470, prevents diet-induced and genetic obesity in mice. Circ Res 94:1579–1588
22. **Sunderkötter C, Steinbrink K, Goebeler M, Bhardwaj R, Sorg C** 1994 Macrophages and angiogenesis. J Leukoc Biol 55:410–422
23. **Pang C, Gao Z, Yin J, Zhang J, Jia W, Ye J** 2008 Macrophage infiltration into adipose tissue may promote angiogenesis for adipose tissue remodeling in obesity. Am J Physiol Endocrinol Metab 295:E313–E322
24. **Cinti S, Mitchell G, Barbatelli G, Murano I, Ceresi E, Faloia E, Wang S, Fortier M, Greenberg AS, Obin MS** 2005 Adipocyte death defines macrophage localization and function in adipose tissue of obese mice and humans. J Lipid Res 46:2347–2355
25. **Cheng HL, Mostoslavsky R, Saito S, Manis JP, Gu Y, Patel P, Bronson R, Appella E, Alt FW, Chua KF** 2003 Developmental defects and

Downloaded from https://academic.oup.com/endo/article/153/4/1706/2423847 by guest on 23 April 2024

p53 hyperacetylation in Sir2 homolog (SIRT1)-deficient mice. Proc Natl Acad Sci USA 100:10794–10799
26. **Gao Z, Wang Z, Zhang X, Butler AA, Zuberi A, Gawronska-Kozak B, Lefevre M, York D, Ravussin E, Berthoud HR, McGuinness O, Cefalu WT, Ye J** 2007 Inactivation of PKCθ leads to increased susceptibility to obesity and dietary insulin resistance in mice. Am J Physiol Endocrinol Metab 292:E84–E91
27. **Gao Z, Ye J** 2008 Inhibition of transcriptional activity of c-JUN by SIRT1. Biochem Biophys Res Commun 376:793–796
28. **Nishimura S, Manabe I, Nagasaki M, Hosoya Y, Yamashita H, Fujita H, Ohsugi M, Tobe K, Kadowaki T, Nagai R, Sugiura S** 2007 Adipogenesis in obesity requires close interplay between differentiating adipocytes, stromal cells, and blood vessels. Diabetes 56: 1517–1526
29. **Van Rooijen N, Sanders A** 1994 Liposome mediated depletion of macrophages: mechanism of action, preparation of liposomes and applications. J Immunol Methods 174:83–93
30. **Gao Z, He Q, Peng B, Chiao PJ, Ye J** 2006 Regulation of nuclear translocation of HDAC3 by IκBa is required for tumor necrosis factor inhibition of peroxisome proliferator-activated receptor γ function. J Biol Chem 281:4540–4547
31. **Sun K, Kusminski CM, Scherer PE** 2011 Adipose tissue remodeling and obesity. J Clin Invest 121:2094–2101
32. **Takeda N, O'Dea EL, Doedens A, Kim JW, Weidemann A, Stockmann C, Asagiri M, Simon MC, Hoffmann A, Johnson RS** 2010 Differential activation and antagonistic function of HIF-α isoforms in macrophages are essential for NO homeostasis. Genes Dev 24: 491–501
33. **Lumeng CN, Bodzin JL, Saltiel AR** 2007 Obesity induces a phenotypic switch in adipose tissue macrophage polarization. J Clin Invest 117:175–184
34. **Yang SR, Wright J, Bauter M, Seweryniak K, Kode A, Rahman I** 2007 Sirtuin regulates cigarette smoke induced pro-inflammatory mediators release via RelA/p65 NF-κB in macrophages in vitro and in rat lungs in vivo. Am J Physiol Lung Cell Mol Physiol 292:L567–L576
35. **Yoshizaki T, Schenk S, Imamura T, Babendure JL, Sonoda N, Bae EJ, Oh DY, Lu M, Milne JC, Westphal C, Bandyopadhyay G, Olefsky JM** 2010 SIRT1 inhibits inflammatory pathways in macrophages and modulates insulin sensitivity. Am J Physiol Endocrinol Metab 298:E419–E428
36. **Schug TT, Xu Q, Gao H, Peres-da-Silva A, Draper DW, Fessler MB, Purushotham A, Li X** 2010 Myeloid deletion of SIRT1 induces inflammatory signaling in response to environmental stress. Mol Cell Biol 30:4712–4721
37. **Brunet A, Sweeney LB, Sturgill JF, Chua KF, Greer PL, Lin Y, Tran H, Ross SE, Mostoslavsky R, Cohen HY, Hu LS, Cheng HL, Jedrychowski MP, Gygi SP, Sinclair DA, Alt FW, Greenberg ME** 2004 Stress-dependent regulation of FOXO transcription factors by the SIRT1 deacetylase. Science 303:2011–2015
38. **Motta MC, Divecha N, Lemieux M, Kamel C, Chen D, Gu W, Bultsma Y, McBurney M, Guarente L** 2004 Mammalian SIRT1 represses forkhead transcription factors. Cell 116:551–563
39. **Langley E, Pearson M, Faretta M, Bauer UM, Frye RA, Minucci S, Pelicci PG, Kouzarides T** 2002 Human SIR2 deacetylates p53 and antagonizes PML/p53-induced cellular senescence. EMBO J 21: 2383–2396
40. **Cho CH, Koh YJ, Han J, Sung HK, Jong Lee H, Morisada T, Schwendener RA, Brekken RA, Kang G, Oike Y, Choi TS, Suda T, Yoo OJ, Koh GY** 2007 Angiogenic role of LYVE-1-positive macrophages in adipose tissue. Circ Res 100:e47–e57
41. **Herbert SP, Stainier DY** 2011 Molecular control of endothelial cell behaviour during blood vessel morphogenesis. Nat Rev Mol Cell Biol 12:551–564
42. **Bouloumié A, Drexler HC, Lafontan M, Busse R** 1998 Leptin, the product of Ob gene, promotes angiogenesis. Circ Res 83:1059–1066
43. **Cao R, Brakenhielm E, Wahlestedt C, Thyberg J, Cao Y** 2001 Leptin induces vascular permeability and synergistically stimulates angiogenesis with FGF-2 and VEGF. Proc Natl Acad Sci USA 98:6390–6395
44. **Ouchi N, Kobayashi H, Kihara S, Kumada M, Sato K, Inoue T, Funahashi T, Walsh K** 2004 Adiponectin stimulates angiogenesis by promoting cross-talk between AMP-activated protein kinase and Akt signaling in endothelial cells. J Biol Chem 279:1304–1309
45. **Bråkenhielm E, Veitonmäki N, Cao R, Kihara S, Matsuzawa Y, Zhivotovsky B, Funahashi T, Cao Y** 2004 Adiponectin-induced antiangiogenesis and antitumor activity involve caspase-mediated endothelial cell apoptosis. Proc Natl Acad Sci USA 101:2476–2481
46. **Greenberg JI, Shields DJ, Barillas SG, Acevedo LM, Murphy E, Huang J, Scheppke L, Stockmann C, Johnson RS, Angle N, Cheresh DA** 2008 A role for VEGF as a negative regulator of pericyte function and vessel maturation. Nature 456:809–813
47. **Potente M, Gerhardt H, Carmeliet P** 2011 Basic and therapeutic aspects of angiogenesis. Cell 146:873–887
48. **Boucher J, Masri B, Daviaud D, Gesta S, Guigné C, Mazzucotelli A, Castan-Laurell I, Tack I, Knibiehler B, Carpéné C, Audigier Y, Saulnier-Blache JS, Valet P** 2005 Apelin, a newly identified adipokine up-regulated by insulin and obesity. Endocrinology 146:1764–1771

Downloaded from https://academic.oup.com/endo/article/153/4/1706/2423847 by guest on 23 April 2024